

# Software configurable optical test system: a computerized reverse Hartmann test

Peng Su,<sup>1,\*</sup> Robert E. Parks,<sup>1</sup> Lirong Wang,<sup>1</sup> Roger P. Angel,<sup>1,2</sup> and James H. Burge<sup>1,2</sup>

<sup>1</sup>College of Optical Sciences, The University of Arizona, Tucson, Arizona 85721, USA

<sup>2</sup>Department of Astronomy/Steward Observatory, The University of Arizona, Tucson, Arizona 85721, USA

\*Corresponding author: psu@email.arizona.edu

Received 11 March 2010; revised 10 July 2010; accepted 14 July 2010;  
posted 16 July 2010 (Doc. ID 125262); published 5 August 2010

A software configurable optical test system (SCOTS) based on the geometry of the fringe reflection or phase measuring deflectometry method was developed for rapidly, robustly, and accurately measuring large, highly aspherical shapes such as solar collectors and primary mirrors for astronomical telescopes. In addition to using phase shifting methods for data collection and reduction, we explore the test from the point view of performing traditional optical testing methods, such as Hartmann or Hartmann–Shack tests, in a reverse way. Using this concept, the slope data calculation and unwrapping in the test can also be done with centroiding and line-scanning methods. These concepts expand the test to work in more general situations where fringe illumination is not practical. Experimental results show that the test can be implemented without complex calibration for many applications by taking the geometric advantage of working near the center curvature of the test part. The results also show that the test has a large dynamic range, can achieve measurement accuracy comparable with interferometric methods, and can provide a good complement to interferometric tests in certain circumstances. A variation of this method is also useful for measuring refractive optics and optical systems. As such, SCOTS provides optical manufacturers with a new tool for performing quantitative full field system evaluation. © 2010 Optical Society of America

*OCIS codes:* 080.4228, 120.6650, 150.3045.

## 1. Introduction

The software configurable optical test system (SCOTS) is a simple, inexpensive, yet highly flexible optical test that can be configured with software for almost any specular surface or lens system. In its simplest configuration, all that is needed to perform the test is a laptop computer with a built-in camera. The laptop illuminates the test surface with a light pattern on the LCD screen and uses the reflected image to determine the surface gradients.

The idea of SCOTS goes back to the only tests opticians had for measuring topography prior to the laser and computers, namely, slope measuring tests such as the Foucault knife edge, the Ronchi test, which can be thought of as several knife positions

captured in a single image, and the Hartmann test, which was used to figure the 5 m Mount Palomar primary mirror among others [1–3]. The work described here was started independently from other work that dates back to at least 1954 in the German mechanical engineering literature [4] and has continued to the present [5–12]. We developed SCOTS for measuring solar concentrators and mirrors for astronomical telescopes at different stages of fabrication. This field is already rich with similar applications of slope measurements for everything from three-dimensional shapes of specular surfaces such as car bodies to progressive eyeglasses. There are patented applications of the method [13] and some commercial products [14,15].

Our contribution to this field is the specific hardware and algorithms optimized for measuring optical surfaces and systems, utilizing the geometry to achieve high-performance results with loose

---

0003-6935/10/234404-09\$15.00/0  
© 2010 Optical Society of America

tolerances. By measuring optical surfaces from their center of curvature, we take advantage of the relaxation for geometric calibration to achieve high measurement accuracy, because the measurement configuration is close to stigmatic. Furthermore, while the fundamental method has been known for over 50 years, it has only been in the last few years that technology has advanced to the point where it is possible to economically implement the method and get wavefront measurements comparable in precision to traditional phase shifting interferometry. Again, 1 nm or better sensitivity has been pointed out in the literature [12] but only over small samples, and not as applied to measuring form errors for large optics. This application relies on the excellent sensitivity that can be achieved by phase shift or centroid techniques and the extremely high dynamic range provided by modern displays. For example, the separation between individual pixels in a 10 in.  $\times$  13 in. display is  $\sim 260 \mu\text{m}$ . The accuracy of the position of these pixels is around 1% of the pitch, so the off-the-shelf display provides measurements with a dynamic range of about 10 parts per million.

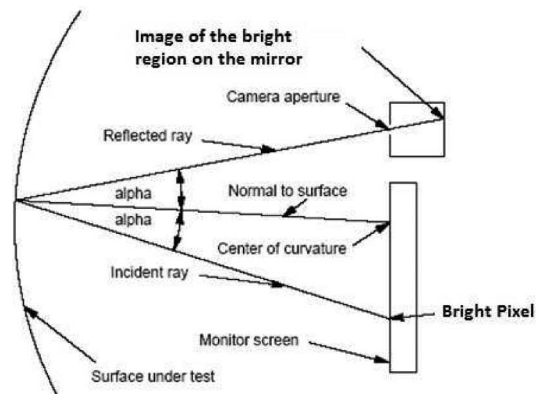
In this paper, we first describe the principle of SCOTS as a Hartmann test [3] in reverse with the introduction of the centroiding calculation model and the line scan unwrapping method. Then experimental results of measuring a 130 mm off-axis parabolic mirror (OAP), a 1 m solar reflector segment, and the 8.4 m diameter off-axis segment for the Giant Magellan Telescope (GMT) are presented. The test results show that the test can be implemented without complex calibration for many applications; it can achieve measurement accuracy comparable with interferometric methods and can provide an excellent complement for interferometric measurements. We also discuss using SCOTS for measuring refractive optical systems and provide a comparison between the centroiding method and the phase shifting method used in phase modulation deflectometry (PMD).

## 2. SCOTS Principle

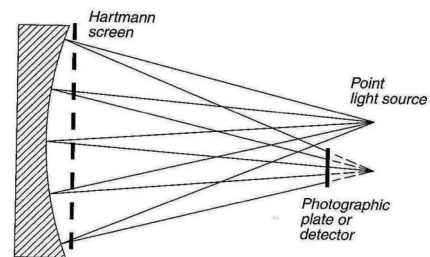
### A. Reverse Hartmann Test Model

The testing of solar concentrators presents an unusual problem in optical testing because the required quality of the concentrator falls in a middle ground between precision optics and architectural glazings. Further, the test hardware must be inexpensive and compatible with rapid, low cost manufacturing methods. It was these requirements that led Roger Angel [16] of Steward Observatory at the University of Arizona to suggest the SCOTS method as a means of testing the solar concentrators that he was embarking on making at the Steward Observatory Mirror Laboratory. He envisioned using a laptop with a built-in camera to realize his requirements. If a single pixel is lit up on the otherwise dark screen, the image of the mirror, made with the camera CCD detector, will show a bright region corresponding to the areas on the mirror with a particular range of slopes, as shown

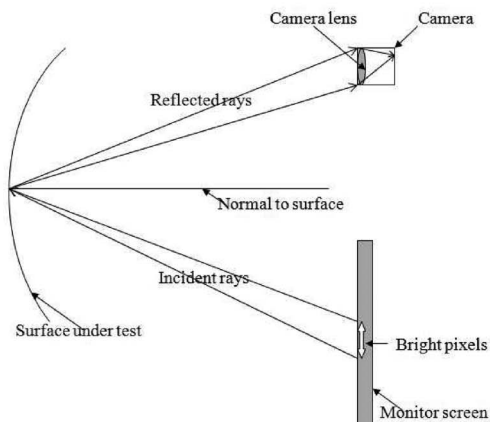
in Fig. 1(a). Using a pinhole camera model (distortion in the camera lens can be calibrated and corrected during the data reduction with common camera calibration methods used in computer vision science [17]) and the law of reflection, the part of the mirror where the angle of incidence of the light from the screen is equal to the angle of reflection back to the camera will appear bright in the picture. The angular bisector of these two rays is normal to the surface at the bright area. The surface slopes ( $w_x$  and  $w_y$ ) can be calculated by knowing the locations of the lit pixel on the screen, the camera and the mirror bright region as shown in the differential Eq. (1). The slopes can be integrated using a polynomial fit to the slopes or by zonal



(a)



(b)



(c)

Fig. 1. Geometry of (a) SCOTS, (b) Hartmann test, and (c) multiple screen pixels lighting up the same mirror pixel.

integration methods [3,18] to give the surface shape ( $w$ ):

$$\begin{aligned} w_x(x_m, y_m) &= \frac{\frac{x_m - x_{\text{screen}}}{d_{m2\text{screen}}} + \frac{x_m - x_{\text{camera}}}{d_{m2\text{camera}}}}{\frac{z_{m2\text{screen}} - w(x_m, y_m)}{d_{m2\text{screen}}} + \frac{z_{m2\text{camera}} - w(x_m, y_m)}{d_{m2\text{camera}}}}, \\ w_y(x_m, y_m) &= \frac{\frac{y_m - y_{\text{screen}}}{d_{m2\text{screen}}} + \frac{y_m - y_{\text{camera}}}{d_{m2\text{camera}}}}{\frac{z_{m2\text{screen}} - w(x_m, y_m)}{d_{m2\text{screen}}} + \frac{z_{m2\text{camera}} - w(x_m, y_m)}{d_{m2\text{camera}}}}, \end{aligned} \quad (1)$$

where  $x_m$  and  $y_m$  are the coordinates of the test surface that can be obtained from the calibrated mirror image (bright region);  $x_{\text{camera}}$  and  $y_{\text{camera}}$  are the coordinates of the camera that can be obtained from geometric measurement of the test setup;  $x_{\text{screen}}$  and  $y_{\text{screen}}$  are the coordinates of the bright screen pixel that can be calculated by centroiding or phase shifting methods as discussed below;  $z_{m2\text{screen}}$  and  $z_{m2\text{camera}}$  are the  $z$  coordinate differences between the mirror and the screen and between the mirror and the camera;  $d_{m2\text{screen}}$  and  $d_{m2\text{camera}}$  are the distances between the mirror and the screen and between the mirror and the camera; and  $z_{m2\text{screen}}$ ,  $z_{m2\text{camera}}$ ,  $d_{m2\text{screen}}$ , and  $d_{m2\text{camera}}$  can be obtained from geometric measurement and calibration.

Using the SCOTS test is analogous to doing a traditional Hartmann test, with the light going through the system in reverse. As shown in Fig. 1(b), in a Hartmann test a point source of light at the center of the curvature reflects off the surface being tested. The pupil is divided into numerous sample regions with a mask, and the light from each of these regions refocuses on a detector. The positions of the refocused light spots indicate the slope of the surface in each of the regions, and these slopes can be compared with those for a theoretically perfect surface. In SCOTS, it is useful to visualize the system backward, where the rays start from the camera aperture, hit the mirror, and reflect to the screen. Now the screen has the function of the detector in the Hartmann test, while the camera works as the point source. Moreover, because the camera takes the pictures of the mirror during the test, it also supplies information about the pupil coordinates (measurement positions at the mirror), which correspond to the Hartmann screen hole positions. Each illuminated camera pixel samples a certain region of the test mirror. We call this region the mirror pixel for convenience in the following discussions. With a finite size of the camera aperture, multiple screen pixels can light up the same mirror pixel, as shown in Fig. 1(c). Analogous to the Hartmann test, the average slope at a mirror pixel can be measured by evaluating the centroid (first moments) of the corresponding screen pixels [19] with Eq. (2) and then substituting the centroid values back into Eq. (1):

$$x_{\text{screen}} = \frac{\sum_{i \in \text{ESP}} x_i I_i}{\sum_{i \in \text{ESP}} I_i}, \quad y_{\text{screen}} = \frac{\sum_{i \in \text{ESP}} y_i I_i}{\sum_{i \in \text{ESP}} I_i}, \quad (2)$$

where the centroid of the screen pixels ( $x_{\text{screen}}$ ,  $y_{\text{screen}}$ ) can be calculated from a light intensity weighted average using effective screen pixels (ESPs). The ESPs are all the pixels that can light up a certain mirror pixel. Pixel light intensities can be read out from the camera pictures. In practice, to get enough light signal and better centroiding, instead of closing the iris of the camera to a pinhole, which can be good for filtering out all the unwanted light, however suffering significant diffraction effects from the camera lenses, a finite aperture that leads to a 3–5 screen pixels per mirror pixel sampling is used. This is analogous to the sampling in a Hartmann/Hartmann–Shack (H/H-S) test [20].

## B. Data Collection and Unwrapping

An intuitive way to run this test is lighting up a single screen pixel, taking a picture of the mirror, finding the corresponding illuminated mirror pixels, repeating the above procedure until covering the full mirror, and then calculating the surface slopes with Eqs. (1) and (2). However, the pixel-by-pixel method is slow for measuring a whole surface. To speed up the test, multiple pixels should be lit up at one time. However, when several arbitrary pixels are lit up simultaneously on the screen, multiple mirror pixels may be lit up by the light from those screen pixels, and we will have mapping ambiguities between the screen pixels and the mirror pixels, so that the surface slope cannot be calculated with certainty. With the assumption that the sag of the test surface is much smaller than the distance between the surface and the camera or the screen, the coupled first-order differential Eq. (1) can then be reduced to Eqs. (3):

$$\begin{aligned} w_x(x_m, y_m) &= \frac{\frac{x_m - x_{\text{screen}}}{z_{m2\text{screen}}} + \frac{x_m - x_{\text{camera}}}{z_{m2\text{camera}}}}{2}, \\ w_y(x_m, y_m) &= \frac{\frac{y_m - y_{\text{screen}}}{z_{m2\text{screen}}} + \frac{y_m - y_{\text{camera}}}{z_{m2\text{camera}}}}{2}. \end{aligned} \quad (3)$$

From Eqs. (3), the ambiguity issue can be solved by requiring the screen pixels be lit up as a line in the  $x$  or  $y$  direction. The surface  $x$  or  $y$  slope at a certain mirror pixel can be determined without needing to know both the  $x$  and the  $y$  coordinates of the screen pixels. By scanning line by line in  $x$  and then in  $y$ , the full mirror surface slopes can be obtained. To further speed up the test, it is possible to scan multiple lines simultaneously with different intensities. The mapping ambiguities between lines are solved by the intensity coding. Sinusoidal fringes can be generated on the screen and used for illuminating the test surface. By phase shifting the fringes and taking pictures, the phase value that corresponds to a screen pixel coordinate at a certain mirror pixel can be found by synchronous detection techniques. This is where the phase shifting methods for the fringe reflection come from. The light intensity from the screen entering the aperture of the camera can be described as

$$I = a + b \cos(2\pi r/p + t), \quad (4)$$

where  $a$  and  $b$  are the background intensity and amplitude modulation, respectively,  $r$  is the screen pixel coordinate,  $p$  is the period of the sinusoidal fringe,  $2\pi r/p$  is the phase to be found, and  $t$  is the additional phase shift. For example, in a four-step phase shifting algorithm,  $t$  can be  $0, \pi/2, \pi,$  and  $3\pi/2$  and is controlled by adjusting the light intensity of the screen pattern. Four images of the mirror are collected. If we call the intensity values at each mirror pixel as  $I_1, I_2, I_3,$  and  $I_4$ , then the phase value  $2\pi r/p$  can be calculated as in Eq. (5):

$$2\pi r/p = \arctan \left[ \frac{I_4 - I_2}{I_1 - I_3} \right]. \quad (5)$$

Using Eqs. (4) and (5), the position  $r$  on the screen related with a certain mirror pixel can be determined. When more than one screen pixel illuminates the same mirror pixel, Eqs. (4) and (5) mathematically will give the averaged phase because  $I_1, I_2, I_3,$  and  $I_4$  are the sum of the intensities from those screen pixels.

Mapping ambiguities may still exist when more than one fringe is used for measuring the full test surface. This is exactly the same phase unwrapping issue faced in the interferogram analysis. In the literature of PMD, this phase unwrapping ambiguity is commonly solved by using fringes with multiple periods [21]. The test starts with a long period fringe and then reduces the fringe periods to increase the test accuracy. However, the limitation to this unwrapping technique is that the usable screen size for testing is limited by the screen region covered by one fringe. Many commercial LCD displays only have 256 light intensity levels. The  $256 \times 2 \times$  screen pixel pitch will be the usable screen region without any phase ambiguity. Scanning the fringe is needed to further increase the dynamic range.

Under the concept of the centroiding method, SCOTS uses a brute force method to solve the phase ambiguity issue in the time domain. This way, many phase unwrapping problems encountered in the interferogram analysis can be avoided [22]. Fundamentally, the unwrapping issue is to find the mapping relationship between the mirror pixels and the corresponding screen pixels. If each time the test mirror is illuminated with one line of screen pixels and the illuminated mirror pixels are located, the mapping relation is uniquely determined. So scanning line by line with a threshold value for throwing away noisy data supplies a brute force solution to this unwrapping issue in a SCOTS test. Similar to multiple-period methods and other temporal phase unwrapping algorithms, the line-scanning method solves the unwrapping issue in the time domain. The multiple-period methods use several fringe periods based on the noise in the phase data, because phase errors in the measurement with long period fringes sometimes can be bigger than the period used

by the measurement with short period fringes. The phase ambiguity issue will still exist if there are no measurements with intermediate periods. Unwrapping with the line-scanning method does not suffer from the effects induced by phase errors in any way and has no dynamic range limitation compared to the multiple-period methods. However, it does take more time to collect the data.

For many precision measurements or when the test surface is fast, the simplifications in Eq. (3) are no longer tolerable. This requires us to go back to Eq. (1). In Eq. (1), slopes are functions of the surface shape ( $w(x_m, y_m)$ ) itself. For many optical applications, a CAD model or measurements from other test methods can supply a good initial estimate of the surface shape. The integrated sag from the slope calculations can be put back into Eq. (1) to iteratively calculate the slopes and sags the same way as commonly used to solve differential equations. Equation (1) also requires knowing the locations of the lit pixel on the screen. This can be obtained after the mapping between the mirror pixel and the screen pixel in both the  $x$  and the  $y$  directions is calculated from line-scanning unwrapping or phase unwrapping as explained above.

### C. Camera Mapping and Solving Ambiguity Due to Surface Sag Discontinuities

Based on Eq. (1), mapping between the pixel coordinates of the camera and the object surface coordinates also needs to be accurately established to achieve the required measurement accuracy. This can be done by photogrammetric methods used in computer vision science [17]. For many applications, a careful tolerance analysis is needed. The sensitivity to the camera lens distortion is greatly reduced when measuring an optic at its center of curvature. For example, if both the camera and the screen are at the center of the curvature of a sphere, it is near a stigmatic test. This type of test is largely insensitive to the position measurement information of the camera (the mapping between the pixel coordinates of the camera and the object surface coordinates). When measuring an optic in an off-axis configuration because the camera and screen usually need to be physically separated, an oblate ellipse will be its own stigmatic-test configuration. The derivative of the test surface departure from an ellipse will reflect the sensitivity of the camera distortion effect.

Because SCOTS is a slope measurement technique, it suffers an ambiguity when the object under test has surface discontinuities. This can be solved by shifting the screen or using multiple cameras [23]. Another engineering approach to solve this sag ambiguity issue is using SCOTS with a commercial one-dimensional (1D) displacement sensor [24]. This kind of sensor is a 1D version of the fringe projection devices; however, it can be used for measuring both specular and diffusive surfaces due to its unique imaging geometry. The displacement sensor can provide the relationships between the isolated test regions.

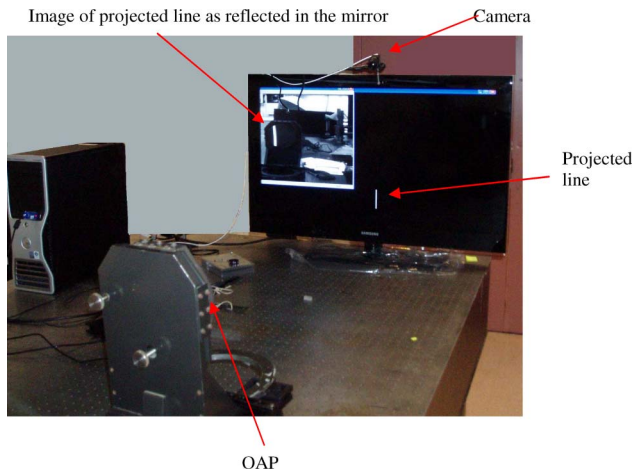


Fig. 2. (Color online) Hardware setup used to perform a SCOTS test.

### 3. Experiments

#### A. SCOTS for Off-Axis Parabolic Mirror

We tested SCOTS performance initially by measuring a 130 mm diameter off-axis parabola (OAP). Its parent radius of curvature was  $\sim 1288$  mm, and the off-axis distance was  $\sim 206$  mm. Figure 2 shows the experimental setup. A 42 in. LCD TV screen (much larger than needed for this measurement), a CCD camera, and a computer are the basic components for SCOTS. The screen and the camera were located close to the center curvature of the mirror. There is no tight requirement for positioning the screen and the camera as long as their positions can be measured. The camera was pointed at the mirror. The mirror tip/tilt was adjusted slightly so that light from the screen was reflected back into the camera. A coordinate system based on the screen was used for the test. The coordinates of the CCD camera and the mirror were obtained with a tape measure. Figures 3(a) and 3(b) show the slope data calculated from the collected images. Figure 4(a) shows the reconstructed surface shape, and Fig. 4(b) shows the surface aspheric departure from a sphere. Table 1 gives a compar-

ison of SCOTS test results with the mirror shape information from its nominal design value. The surface figure of the off-axis parabola was about 1.6 mm peak to valley. Without any effort to calibrate the test geometry and camera distortion effect,  $1\ \mu\text{m}$  rms or better accuracy was achieved. A numerical tolerance analysis of the alignment (test geometry) and random noise effects was performed, given the coordinate uncertainties of the camera, the mirror, and the screen. The result shows that the test to first order is insensitive to the global coordinate information, as shown in Table 2. This is expected, as most of the global position uncertainties only introduce tilts and power to the surface shape. Here tilts and power are treated as alignment terms, as done by most of the optical testing methods. The slope measurement sensitivity in the test is  $\sim 20\ \mu\text{rad}$  or better, as shown in Eq. (6). With a spatial sampling of 1 mm on the test mirror by the camera, a sag resolution of  $\sim 20$  nm is obtained. The test error is dominated by some systematic errors, and it is possible that the surface itself actually owns those departures from the nominal. We will address these issues in detail in a future work.

The slope resolution is  $\Delta\theta = 0.5 \times \text{subscreen pixel/distance between the screen and the mirror}$ , or

$$\Delta\theta = \frac{0.5\ (\text{mm})/10}{1288\ (\text{mm})} \times 0.5 = 20\text{e} - 6\ \text{rad}, \quad (6)$$

where the screen pixel size is  $\sim 0.5$  mm and we used 1/10 pixel uncertainty in the centroiding or phase shifting calculation, which is a function of the signal-to-noise ratio under the test environment (it can go up to 1/100 pixel or even better, as in the interferogram analysis and H-S test). The factor 0.5 is due to testing the mirror in reflection. In this test, the centroiding and line-scanning methods were used to collect and reduce the data.

#### B. SCOTS for Solar Reflectors

We utilized SCOTS to measure a slumped solar reflector segment [25], an off-axis section of a 3 m,

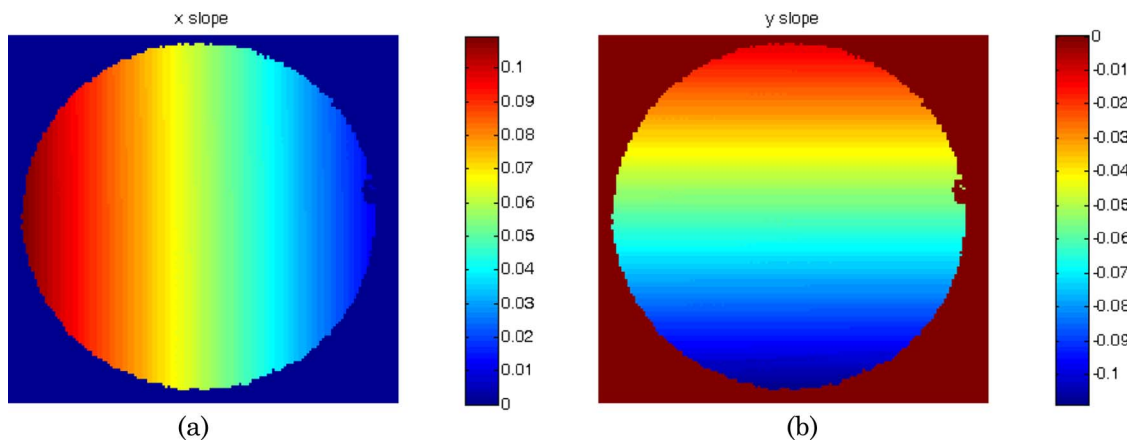


Fig. 3. (Color online) (a)  $x$ -slope data from a 130 mm diameter OAP and (b) corresponding  $y$ -slope data (color bar units are radians).

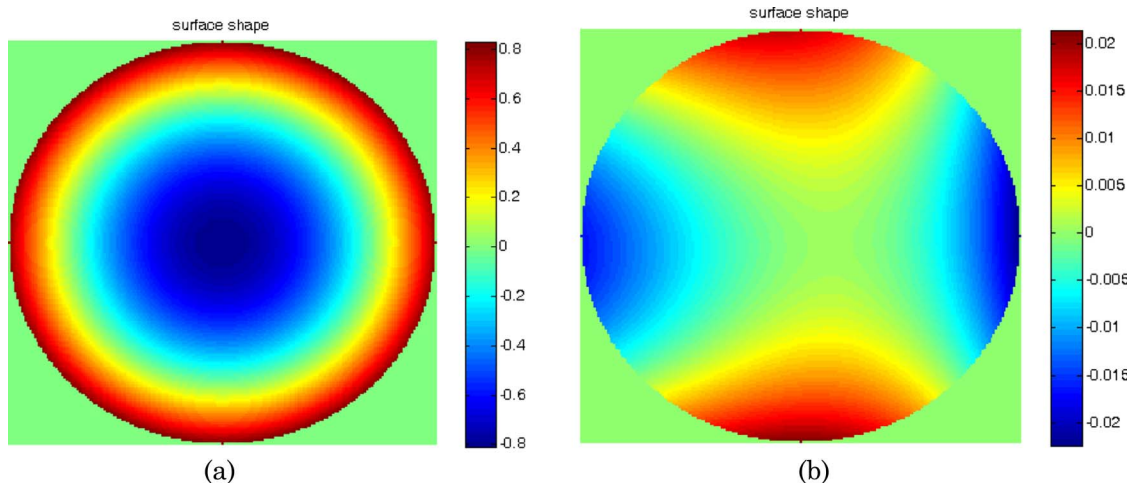


Fig. 4. (Color online) (a) Reconstructed surface shape from SCOTS data and (b) the surface aspheric departure (color bar units are millimeters).

$f/0.5$  parabola, as shown in Fig. 5(a). The segment has a trapezoidal shape about 1 m long by 85 cm at the long end. The monitor was set up close to the center of curvature of the segment roughly aligned perpendicular to the normal at the center of the segment. The camera was located at the edge of the screen. Figures 5(b)–5(e) show the fringe patterns at the screen and some of the raw mirror fringe images from SCOTS. After the tilts, power, and shapes described by the first 11 Zernike standard polynomials [26] were subtracted, the  $x$  and  $y$  slopes are shown in Figs. 6(a) and 6(b). Figure 6(c) shows the mirror shape (low order shape removed) from

slope integration with the Southwell zonal method [18]. The high-frequency shape information obtained from the test is especially useful for improving the mirror fabrication process. Low order shape data were further reduced by fitting with a best fit parabola to get the mirror radius of curvature and the off-axis distance. The test results shown here were obtained with the centroiding and line-scanning method. Media 1, created from the experiment data, shows that the SCOTS test can also be viewed as a reverse wire test where, instead of measuring longitudinal aberration, transverse aberration is measured. Measurement of the full 3 m segmented

Table 1. Comparison of Off-Axis Parabolic Mirror Surface Coefficients from SCOTS and from Its Nominal Values

Surface Shape (Zernike Standard Polynomial) [26]	Coefficients from Test Results (mm rms)	Coefficients Calculated from Nominal Value of the Mirror (mm rms)
Piston	0	0
Tilt $x$	0 (alignment)	0
Tilt $y$	0 (alignment)	0
Power	0.4675 (alignment)	0.4675
Sine astigmatism	-0.0006	unknown
Cosine astigmatism	-0.0080	$\sim -0.0085$
Sine coma	-0.0010	$\sim -0.0015$
Cosine coma	-0.0003	unknown
Sine trefoil	0.0003	unknown
Cosine trefoil	0.0001	unknown
Spherical aberration	0.0000	unknown

Table 2. Tolerance for 130 mm Off-Axis Parabolic Mirror (Surface Errors in Unit of  $\mu\text{m}$  rms)

20 $\mu\text{rad}$ noise in slope data	0.011 power, 0.023 astigmatism, 0.010 coma, and 0.016 trefoil
1 mm mirror $x$ position uncertainty	0.08 astigmatism
1 mm mirror $y$ position uncertainty	0.1 power and 0.08 astigmatism
1 mm mirror $z$ position uncertainty	0.35 $\mu\text{m}$ power
1 mm camera $x$ position uncertainty	0.01 power and 0.01 astigmatism
1 mm camera $y$ position uncertainty	0.01 power and 0.01 astigmatism
1 mm camera $z$ position uncertainty	0.17 power and 0.001 astigmatism
1° screen $x$ tilt	0.16 power and 0.006 astigmatism
1° screen $y$ tilt	0.16 power and 0.012 astigmatism
1° screen rotation	0.15 astigmatism

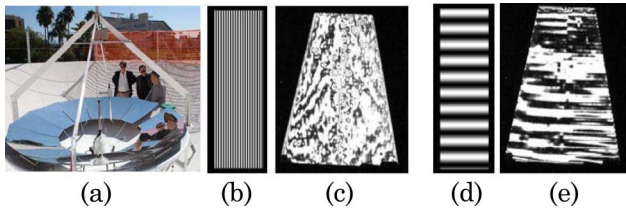


Fig. 5. (Color online) (a) Segmented 3 m,  $f/0.5$  solar concentrator built at the University of Arizona, (b) and (d) are sinusoidal fringes used in SCOTS, (c) and (e) are the corresponding fringe images at a piece of the trapezoidal solar reflector.

mirrors was also done recently with the line-scanning method to accommodate the need of the large screen and the fast slope variations in the solar mirror. The results, details of the experiment setup, and the alignment of the segmented mirrors are reported in Ref. [27].

### C. SCOTS for 8.4 m Giant Magellan Telescope Primary Mirror

After the successful application of SCOTS for solar mirrors, we applied SCOTS to a large optics project where there was difficulty getting good interferometric data at the edge of the steeply aspheric 8.4 m diameter off-axis GMT mirror being polished at the Steward Observatory Mirror Laboratory. The interferometric test used a set of null optics that included a 3.75 m sphere, a 1 m sphere, a computer-generated hologram, and an instantaneous phase shifting interferometer [28]. Everything but the 3.75 m sphere was mounted on an optical bench known as Sam. In order to use SCOTS, the screen and the camera had to be placed above Sam and had to be able to move out of the way when the interferometer was being used. This meant that the circle of least confusion in the screen was about 150 mm in diameter (screen size used in the test), and the camera and screen had to be positioned within about 5 mm laterally to avoid vignetting in the 3.75 m sphere. Camera distortion was calibrated using the cores at the mirror as a reference, as shown in Fig. 7. Once the slopes were obtained and integrated and 24 low-order Zernike terms were removed because the

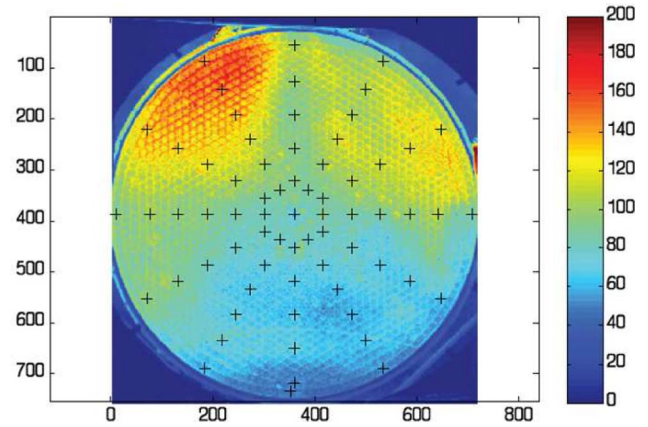


Fig. 7. (Color online) Camera distortion was corrected using cores at the mirror as reference. The image was taken when the environment light was on.

final mirror low-order figure will be controlled with actuators, the integrated surface height map looks like that in Fig. 8(a), while the comparable interferometric data with the same terms removed is shown in Fig. 8(b). Over the central 90% of the diameter of the aperture, the two maps look virtually the same in spatial character and magnitude. At this stage of polishing, the GMT team was glad to have SCOTS data because the slopes were too high at the edge of the mirror to get good interferometric data, and this was exactly where work was needed to improve the surface accuracy. The interferometer could not reliably unwrap the direct phase data at the mirror edge. In this test, both phase shifting and centroiding methods were used, and they gave out equivalent results.

### 4. SCOTS for Refractive Optics

In contrast to the fringe reflection method, we also investigated situations using SCOTS for measuring refractive optics. This is especially useful for measuring or aligning null-lens systems and for aspheric or free-form lenses. In certain senses, SCOTS can provide lens manufacturers with a new tool for lens system evaluation. On-axis performance is measured

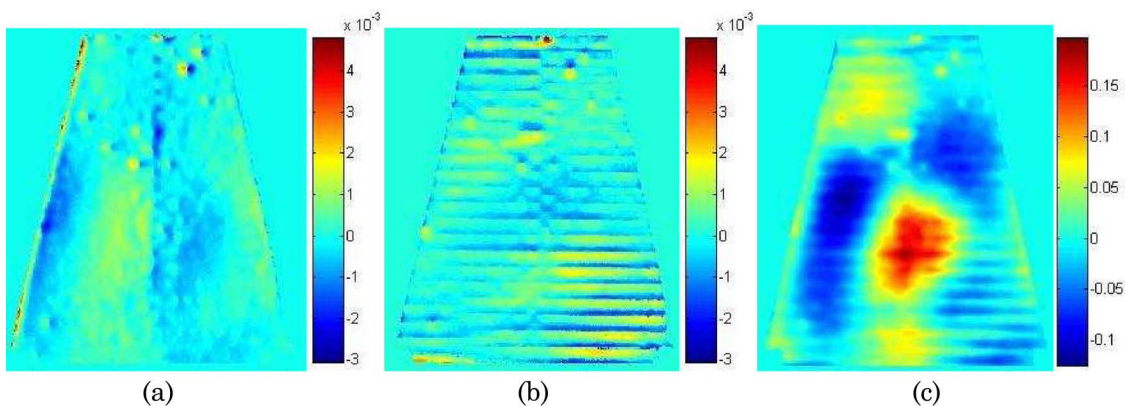


Fig. 6. (Color online) (a)  $x$  slopes of the trapezoidal solar reflector measured with SCOTS (color scale in milliradians), (b)  $y$  slopes, and (c) integrated surface shape after removing overall parabolic shape (color bar scale is in millimeters).

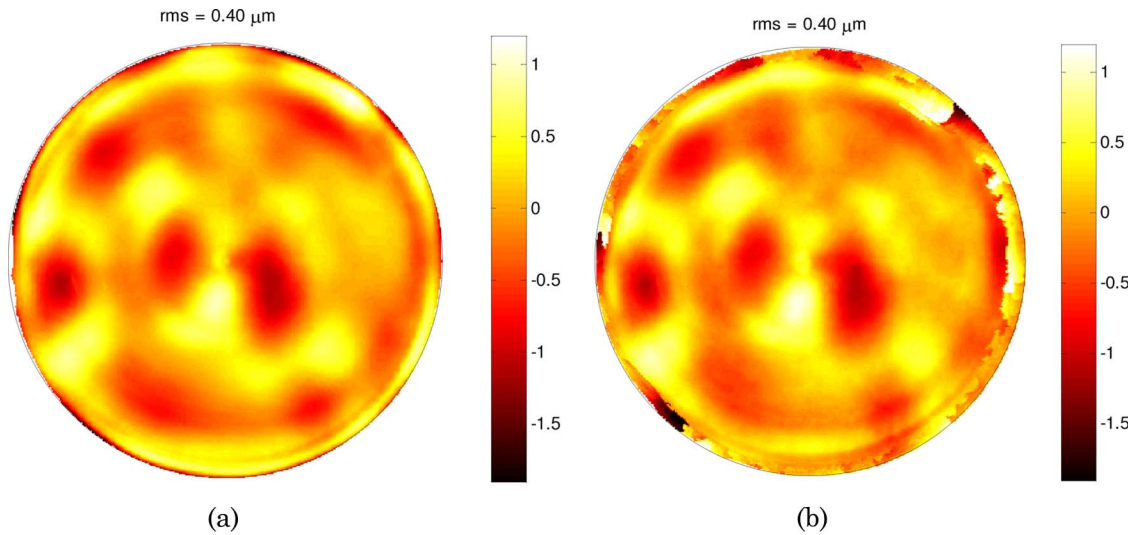


Fig. 8. (Color online) (a) GMT surface data measured by SCOTS and (b) GMT surface data measured interferometrically. The circle represents the 8.4 m clear aperture (color bar units are micrometers).

directly, and off-axis aberrations can be detected as pupil distortions that violate the Abbe sine condition [29]. Figure 9 shows examples of using SCOTS to test a lens system. As in the Hartmann test, transverse ray aberrations are measured by SCOTS and are compared with the theoretical values. Integrating the ray aberrations gives the measure of the wavefront error of the system. To increase the test precision, a finer pitch microdisplay, such as organic light-emitting diode [30] or micro-LCD [31], can be used. With a pixel size of  $15\ \mu\text{m}$ , and 1/100 pixel centroiding, a  $0.15\ \mu\text{m}$  transverse ray aberration measurement precision should match many measurement requirements for various applications. Demonstrations for lens testing are under way.

### 5. Comparison between Centroiding Method and Phase Shifting Method in SCOTS

The mapping relations between the mirror and the screen can be made by centroiding or by using phase shifting. The centroiding method has the advantage of being insensitive to the light variations in the temporal domain, where light intensity changes between each collected mirror image, because this variation induces the same amount of changes to the weighting factors in the centroid calculation, as shown in Eq. (2). The phase shifting algorithm is more sensitive to this variation because the intensity variation will directly induce phase value inconsistency between each phase step, acting as a phase stepping error

in Eqs. (4) and (5). In comparison, the phase shifting algorithm has the advantage of being insensitive to the light variations in the spatial domain where the light varies between screen pixels, because it is an AC measurement. The centroiding method is more sensitive to this variation because the variation contributes different weighting factors to the centroid calculation.

The phase shifting method requires sinusoidal modulation of the light intensity, which makes this method more sensitive to the light intensity linearity of the screen. Certain types of LCD screens show non-linearity, especially at low light levels. Calibration may be needed for an accurate measurement. The centroiding method can use maximum light intensity at each screen pixel during the data collection; this gives a greater signal-to-noise ratio for many test situations. However, because the centroiding calculation is weighted by light intensity, it requires high spatial light uniformity for a high-accuracy measurement.

For the phase shifting method, sinusoidal fringes are used. The fringe contrast will be reduced when we try to use a finer period fringe to increase test sensitivity, because adjacent fringes overlap each other due to the diffraction effect [9]. For the centroiding and line-scanning methods, each time a line is used and data are reduced line by line, so there is no fringe overlapping and washout. One pixel line can be used for measurement if the light intensity is adequate.

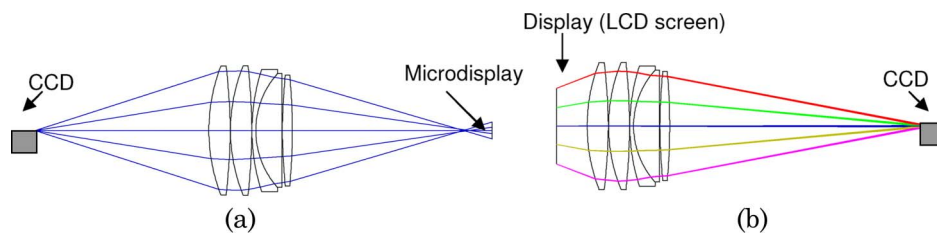


Fig. 9. (Color online) SCOTS setup for measuring lens systems in transmission: measuring (a) imaging performance and (b) pupil distortion.

Because of the average effect in centroiding and phase shifting, both of the two methods will suffer edge effect from the test part. The measurement will be biased because one side of the data does not exist.

## 6. Summary

We show that SCOTS can rapidly and robustly measure large, highly aspherical shapes such as solar collectors and astronomical optics. In addition to phase shifting methods, we explored the fringe reflection method or PMD from a point view of performing a H/H-S test in a reverse way. We solved the slope calculation and unwrapping with centroiding and line-scanning methods. This particular point of view gives us more insight to the nature of the test. Instead of using fringe illumination, centroiding and line-scanning illumination can be a useful solution to an infrared version of SCOTS, where the optics in the grinding stage can look specular and a moving hot wire can generate the test illumination patterns. Moreover, the basics of SCOTS can go back to point illuminations, as explained in Subsection 2.A. We are currently working on using the point version of SCOTS for aligning segmented mirrors in a vacuum chamber.

We gave some initial experimental data of SCOTS. We show that SCOTS can be used without complex calibration and can achieve measurement accuracy comparable with an interferometric test and has great potential for non-null testing. As the test has great sensitivity, further improving the accuracy of the test is one of the goals of our future work. We will also keep investigating the use of SCOTS for measuring refractive optics. This appears especially useful for measuring null-lens systems and aspheric or free-form lenses.

The authors are grateful for the support from the Technology Research Initiative Fund and the Arizona Research Institute for Solar Energy funding from the University of Arizona, and the National Institute of Standards and Technology (NIST), United States Department of Commerce, under ARRA Award 60NANB10D010.

## References

- J. Ojeda-Castañeda, "Foucault, wire, and phase modulation tests," in *Optical Shop Testing*, 3rd ed., D. Malacara, ed., Wiley Series in Pure and Applied Optics (Wiley, 2007), pp. 275–316.
- A. Cornejo-Rodriguez, "Ronchi test," in *Optical Shop Testing*, 3rd ed., D. Malacara, ed., Wiley Series in Pure and Applied Optics (Wiley, 2007), pp. 317–360.
- D. Malacara-Doblado and I. Ghozeil, "Hartmann, Hartmann-Shack, and other screen tests," in *Optical Shop Testing*, 3rd ed., D. Malacara, ed., Wiley Series in Pure and Applied Optics (Wiley, 2007), pp. 361–397.
- F. Ligtenberg, "The moire method, a new experimental method for the determination of moments in small slab models," *Proc. Soc. Exp. Stress Anal.* **12**, 83–98 (1954).
- R. Ritter and R. Hahn, "Contribution to analysis of the reflection grating method," *Opt. Lasers Eng.* **4**, 13–24 (1983).
- D. Perard and J. Beyerer, "Three-dimensional measurement of specular free-form surfaces with a structured-lighting reflection technique," *Proc. SPIE* **3204**, 74–80 (1997).
- R. Diaz-Urbe and M. Campos-García, "Null screen testing of fast convex aspheric surfaces," *Appl. Opt.* **39**, 2670–2677 (2000).
- J. Burke, T. Bothe, W. Osten, and C. Hess, "Reverse engineering by fringe projection," *Proc. SPIE* **4778**, 312–324 (2002).
- M. Knauer, J. Kaminski, and G. Hausler, "Phase measuring deflectometry: a new approach to measure specular free form surfaces," *Proc. SPIE* **5457**, 366–376 (2004).
- T. Bothe, W. Li, C. von Kopylow, and W. Jueptner, "High-resolution 3D shape measurement on specular surfaces by fringe reflection," *Proc. SPIE* **5457**, 411–422 (2004).
- Y. Surrel, "Absolute flatness measurement with 10 nm resolution over a 400 mm field," *Proc. SPIE* **6341**, 634136 (2006).
- W. Jüptner and T. Bothe, "Sub-nanometer resolution for the inspection of reflective surfaces using white light," *Proc. SPIE* **7405**, 740502 (2009).
- For example, G. Haeusler M. Knauer, , and R. Lampalzer, "Method and apparatus for determining the shape and the local surface normals of specular surfaces," U.S. patent 7,532,333 (12 May 2009).
- Ondulo from VISUOL Technologies, Metz, France, [www.visuol.com](http://www.visuol.com).
- CSP Services GmbH, QDec, [www.cspservices.eu/files/downloads/CSPServices\\_OptimizingSolarPower.pdf](http://www.cspservices.eu/files/downloads/CSPServices_OptimizingSolarPower.pdf).
- [www.rehnu.com](http://www.rehnu.com).
- J. Weng, P. Cohen, and M. Herniou, "Camera calibration with distortion models and accuracy evaluation," *IEEE Trans. Pattern Anal. Mach. Intell.* **14**, 965–980 (1992).
- W. H. Southwell, "Wave-front estimation from wave-front slope measurements," *J. Opt. Soc. Am.* **70**, 998–1006 (1980).
- D. R. Neal, J. Copland, and D. Neal, "Shack-Hartmann wavefront sensor precision and accuracy," *Proc. SPIE* **4779**, 148–160 (2002).
- K. A. Winick, "Cramer–Rao lower bounds on the performance of charge-coupled-device optical position estimators," *J. Opt. Soc. Am. A* **3**, 1809–1815 (1986).
- W. Osten, W. Nadeborn, and P. Andrá, "General hierarchical approach in absolute phase measurement," *Proc. SPIE* **2860**, 2–13 (1996).
- J. M. Huntley and H. Saldner, "Temporal phase-unwrapping algorithm for automated interferogram analysis," *Appl. Opt.* **32**, 3047–3052 (1993).
- M. Petz and R. Tutsch, "Reflection grating photogrammetry: a technique for absolute shape measurement of specular free-form surfaces," *Proc. SPIE* **5869**, 58691D (2005).
- [www.keyence.com](http://www.keyence.com).
- R. P. Angel and W. B. Davison, "Solar concentrator apparatus with large, multiple, co-axis dish reflectors," U.S. patent application number 20090277440 (12 November 2009).
- R. J. Noll, "Zernike polynomials and atmospheric turbulence," *J. Opt. Soc. Am.* **66**, 207–211 (1976).
- L. Wang, P. Su, R. E. Parks, Y. Wang, R. P. Angel, J. M. Sasian, and J. H. Burge, "A low-cost, flexible, high dynamic range test for free-form illumination optics," presented at the International Optical Design Conference Jackson Hole, Wyoming, USA, 13–17 June 2010.
- J. H. Burge, L. B. Kot, H. M. Martin, R. Zehnder, and C. Zhao, "Design and analysis for interferometric measurements of the GMT primary mirror segments," *Proc. SPIE* **6273**, 62730M (2006).
- J. H. Burge, C. Zhao, and M. Dubin, "Use of the Abbe sine condition to quantify alignment aberrations in optical imaging systems," presented at the International Optical Design Conference Jackson Hole, Wyoming, USA, 13–17 June 2010.
- [www.emargin.com](http://www.emargin.com).
- [www.kopin.com](http://www.kopin.com).